ORIGINAL RESEARCH

Water accessibility to hydroxyls confined in solid wood cell walls

Emil Engelund Thybring [iD] · **Sara Piqueras** [iD] · **Asghar Tarmian** ·
Ingo Burgert

Abstract The hydrophilicity of wood cell walls derives from the presence of hydroxyls, but their accessibility is restricted by physical confinement from the stiff, solid cell walls. This study examines how this confinement affects water uptake of the accessible hydroxyls by tuning their amount through replacement with various non-hydrophilic functional groups. Results from gravimetrically determined hydroxyl accessibility by deuterium exchange are shown not to correlate with moisture uptake in cell walls under vapour conditions or at water-saturation. Instead, spatial availability for water inside solid cell walls is suggested as the dominant factor in controlling cell wall moisture uptake at given climatic conditions.

Keywords Sorption · Water accessibility · Hydrogen bonding · Chemical modification · Wood

Dedicated to the loving memory of the amazing colleague Hervé Bellanger (1985–2017).

E. E. Thybring (✉) · S. Piqueras
Department of Geosciences and Natural Resource Management, University of Copenhagen, Rolighedsvej 23, 1958 Frederiksberg C, Denmark
e-mail: eet@ign.ku.dk

E. E. Thybring · I. Burgert
Institute for Building Materials, Wood Materials Science, ETH Zürich, Stefano-Franscini-Platz 3, 8093 Zürich, Switzerland

E. E. Thybring · I. Burgert
Cellulose and Wood Materials Laboratory, Empa, Ueberlandstrasse 129, 8600 Dübendorf, Switzerland

A. Tarmian
Department of Wood and Paper Science and Technology, University of Tehran, Karaj, Iran

Introduction

Cellulosic fibres are able to attract and bind water molecules due to their high concentration of hydrophilic functional groups, mainly hydroxyls (OH) (Berthold et al. 1994, 1996, 1998). Several studies on loose cellulosic fibres, e.g. cotton and regenerated

cellulose, have shown that the amount of hydrophilic groups accessible for water is correlated with the moisture content of the material (Gibbons 1953; Guthrie and Heinzelman 1974; Howsmon 1949; Rousselle and Nelson 1971). By chemical reaction, hydrophilic groups can be replaced with entities not attracting water, e.g. replacing hydroxyls with methyl or acetyl groups, hereby reducing the moisture uptake in these materials (Gibbons 1953). When hydroxyls are physically confined in lignified, dense cell walls of wood, the physical environment may influence the uptake of moisture more than the accessibility of hydroxyls. For instance, no correlation between accessibility and moisture content was found for cross-linked cellulose fibres with an otherwise loose structure (Stevens and Smith 1970). For solid wood material, thermal modification has previously been used to examine the relation between hydroxyl accessibility and moisture content. No correlation between these two parameters was found by Rautkari et al. (2013) for thermally modified wood covering a large span in hydroxyl accessibility. On the other hand, Altgen et al. (2018) tuned the moisture conditions during thermal modification to control the degree of crosslinking. They found linear correlations between hydroxyl accessibility and moisture content depending on the degree of crosslinking in the wood. However, thermal modification does not only change the degree of crosslinking between wood polymers but also changes the cell wall nano-porosity (Tjeerdsma et al. 1998), both of which affect cell wall interactions with water. Chemical modifications are more well-defined than thermal modification, and a study of wood modified by acetylation showed a linear correlation between moisture content and hydroxyl accessibility (Popescu et al. 2014). That study did, however, not include other types of chemical modifications, which can cause other patterns of spatial availability and the results can therefore not be interpreted as a definite proof of a general correlation between uptake of moisture and hydroxyl accessibility. This study is the first to describe how different chemical modifications of hydroxyls within the solid cell walls of wood affect their moisture content. The aim is to understand how a combination of chemical modification, physical constraints and hydroxyl accessibility for water influences the moisture content within solid wood cell walls.

Materials and methods

Sample material of Norway spruce (*Picea abies* L.) grown in Switzerland was obtained after kiln-drying and conditioning. Specimens were cut as cuboids with dimensions L × R × T = 5 × 10 × 10 mm^3 for gravimetric accessibility measurements and L × R × T = 15 × 10 × 3 mm^3 for spectroscopic accessibility measurements.

Chemical modification of wood cell walls

Three types of chemical modification of the cell wall chemistry were conducted. These were selected based on chemical similarities in modification approaches, yet distinct differences in their effect on the amount of hydroxyls in the cell walls.

Reactions with carboxylic acid anhydrides (acetylation and hexanoylation) were performed using two differently sized reagents: acetic anhydride and hexanoic anhydride (Hill and Jones 1996; Hill et al. 2009). Sample batches of 8 specimens were treated by vacuum impregnation with a mixture of reagent and pyridine (1:4 by volume) followed by heating at 80 °C for various reaction times to yield different degrees of treatment intensity. Treatments were terminated by pouring off the hot reagent and quenching the reaction in ice-cooled acetone. This was followed by one week of washing in several steps, first several times in an acetone–water (1:1 by volume) mixture and then in pure water. Control specimens were heated in pure pyridine or acetic acid up to 23 h to estimate the maximum mass loss due to extraction of cell wall compounds which was found to be < 2%.

Reaction with caprolactone (polycaprolactone (PCL) modification) was performed by pre-swelling a batch of 22 specimens in anhydrous dimethylformamide (DMF) for 24 h under a nitrogen atmosphere. Hereafter, a mixture of caprolactone monomers with tin(III) octoate catalyst (2% by weight) were added to the reaction flask and left to equilibrate for 23 h followed by heating at 95 °C for 24 h. Treatment was stopped by pouring off hot reagent and washing in several steps in acetone. (Ermeydan et al. 2014b).

Before and after all treatments, dry masses and mass gains, i.e. *R* in gram added mass per gram dry wood (often referred to as weight percent gain or WPG in literature), of specimens were determined after vacuum drying (65 °C, 0 mbar) for 24 h. Based on the

mass loss seen for control specimens and the largest mass gain from modification, the uncertainty of R is estimated to max. 10%. All chemicals were purchased from Sigma Aldrich Chemie GmbH (Buchs, Switzerland).

For each modification, the effect on hydroxyl accessibility and water within cell walls was theoretically assessed by calculation of the hydroxyl substitution and the added molecular volume. The latter was determined based on the dry mass gain from modification R, i.e. gram added per gram dry wood (WPG). Following the methodology of Slonimskii et al. (1970), the molar volume of each modification was calculated, see Table 1. From this, the added molecular volume for each modified batch was found by multiplying mass gain R with molecular volume and dividing with molar mass.

The effect of modification on the hydroxyl accessibility is expected to be caused by both hydroxyl substitution and hydroxyl shielding, see Fig. 1. The previous is caused by the substitution of hydroxyls with another type of functional group as a result of modification. Shielding of remaining hydroxyls within the wood cell walls may arise due to the added functional groups being bulkier than the original hydroxyls. This effect is difficult to theoretically assess, and therefore only the effect of hydroxyl substitution was determined theoretically in this study by

$$\Delta c_{\text{sub}} = \frac{1}{M_{\text{sub}}} \tag{1}$$

where Δc_{sub} (mol g^{-1}) is the expected change in accessibility from hydroxyl substitution per gram mass gain R (g g^{-1}), M_{sub} (g mol^{-1}) is the added
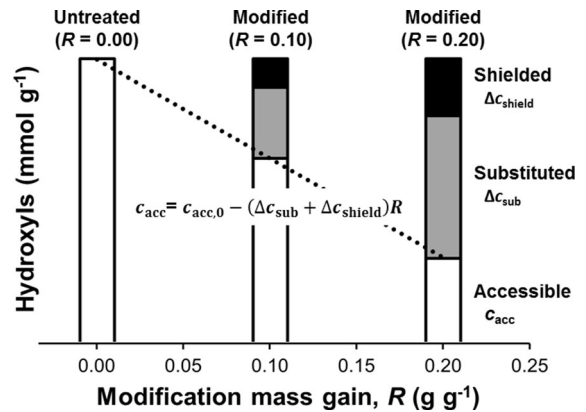

Fig. 1 Schematic illustration of the effects of modification on hydroxyl accessibility: some hydroxyls are substituted by the added functional groups, while others are shielded by these

molar mass of the functional group substituting hydroxyls, which also takes into account mass loss from removal of atom(s). Table 1 clearly illustrates the distinct differences in hydroxyl substitution between the three types of chemical modification.

Characterisation of modification distribution within cell walls

Wood specimens were prepared for Raman imaging according to Gierlinger et al. (2012). Briefly, cross-sections of 15 μm thickness of both untreated and modified wood were cut with a Leica microtome (Leica RM2255). The modified specimens were those with the highest R of the gravimetric specimens in Table 2. The cross-sections were put on glass microscope slides, a couple of water drops were added, glass cover slips were placed on top of the cuts and sealed with nail polish before measurements. Confocal

Table 1 Molar mass, molecular volume and hydroxyl substitution per mass gain, R (g g^{-1}) for added functional groups by modification

Modification	Added functional group	Molar mass added, M_{sub} (g mol^{-1})	Molecular volume, V_{sub} (cm^3 mol^{-1})	Added volume, $V_{\text{sub}}/M_{\text{sub}}$ (cm^3 g^{-1})	Hydroxyl substitution, Δc_{sub} (mmol g^{-1})
Acetylation	–COCH$_3$	42.04	26.0	0.618	23.8
Hexanoylation	–CO(CH$_2$)$_4$CH$_3$	98.14	67.2	0.685	10.2
PCL modification	–(CH$_2$)$_4$COOH	114.14	66.1	0.579	0.0

Volumes based on methodology by Slonimskii et al. (1970). Each treatment removes a hydrogen atom (H) from the hydroxyl with which the modification reacts

Table 2 Overview of modification mass gain, R (g g^{-1}) for the specimens used for gravimetric and spectroscopic measurements

Modification	R (g g^{-1}) for gravimetric specimens	R (g g^{-1}) for spectroscopy specimens
Acetylation	0.126, 0.184, 0.239	0.128, 0.204
Hexanoylation	0.100, 0.143[a], 0.200	0.079, 0.176
PCL modification	0.163	0.181

[a]Only used for cell wall moisture capacity measurement

Raman imaging was performed on both early- and latewood portions of the sample cross-sections. The measurements were performed using a WITec alpha 300 R confocal Raman microscope (WITec Wissenschaftliche Instrumente und Technologie GmbH, Ulm, Germany) equipped with a 532 nm laser, an oil immersion 100× objective (NA 1.4, Carl Zeiss, Jena, Germany). All Raman images were taken with a lateral resolution of 0.3 μm by acquiring at every pixel one spectrum with an integration time of 0.1 s and a laser power of 10 mW.

Data treatment of the Raman imaging data consisted of two consecutive steps: (1) pre-processing of the image spectra to correct fluorescence contribution, and (2) analysis by Multivariate Curve Resolution-Alternating Least Squares (MCR-ALS) to obtain pure spectra of the image constituents and their related distribution maps. The first step consisted in baseline correction by the algorithm Asymmetric Least Squares (Eilers 2004) which has been demonstrated to cope well with fluorescence contribution (Piqueras et al. 2011). Once Raman images are pre-processed, MCR-ALS analysis was performed individually on the untreated, acetylated, hexanoylated and PCL modified Norway spruce wood following the MCR-ALS steps described in the literature (Jaumot et al. 2005). Five and four contributions were needed to describe the variation in the untreated and modified wood, respectively. Each of the MCR-ALS analysis were carried out under the non-negativity constraint in both the concentration and the spectral profiles (Bro and De Jong 1997) and normalization of pure spectra in the $\mathbf{S^T}$ matrix (using 2-norm, i.e., the Euclidean norm).

Water accessibility to hydroxyl groups

Accessibility of hydroxyl groups to water was experimentally probed by deuterium exchange using heavy water (deuterium oxide, D$_2$O). By supplying vast amounts of D$_2$O compared with the amount of hydroxyls in cell walls, those interacting with heavy water exchanged their normal hydrogen (protium) for the heavier isotope (deuterium). Hereby, cell wall dry masses increased with 1 mg per mmol exchanged (Sepall and Mason 1961; Wadehra and Manley 1966) and infrared vibrations of the exchanged hydroxyls shifted by roughly 1000 cm^{-1} (Gold and Satchell 1955; Hofstetter et al. 2006; Mann and Marrinan 1956; Schmidt et al. 2006; Taniguchi et al. 1966; Watanabe et al. 2006). However, about one-third of the hydroxyls on the surface of cellulose microfibrils cannot be deuterium exchanged (Lindh et al. 2016), which corresponds to about 1.3 mmol per gram cellulose (Thybring et al. 2017). Since cellulose makes up roughly half of the composite cell wall, the underestimation of the true hydroxyl accessibility is about 0.7 mmol g^{-1} for untreated wood.

Determination of hydroxyl accessibility by dry mass increase was done gravimetrically using Dynamic Vapour Sorption equipment (DVS-ET1, Surface Measurement Systems, London, UK) at ETH Zürich. Specimens were cut into thin slivers of earlywood and latewood, separately, (mass 5–10 mg, 3 replicates) using a razor blade and exposed to 95% vapour pressure D$_2$O (99.9%-atom purity, Sigma Aldrich Chemie GmbH Buchs, Switzerland) for 10 h which initial experiments had shown was sufficient for full deuteration of the water-accessible hydroxyls. Before and after D$_2$O exposure, each specimen was dried at 60 °C for 6 h using the built-in heating coil followed by a 1 h thermal stabilisation period, all the while purging with dry nitrogen gas. From the measured dry mass increases, the hydroxyl accessibility was calculated as

$$c_{\mathrm{acc}} = \frac{\Delta m_{\mathrm{dry}}}{m_0(M_{\mathrm{D}} - M_{\mathrm{H}})(1 + R)} \qquad (2)$$

where Δm_{dry} (g) is the dry mass increase, m_0 (g) is the initial dry mass, M_D–M_H (g mol^{-1}) is the difference in molar mass between normal (protium) and heavy hydrogen (deuterium), and R (g g^{-1}) is the relative mass gain in the modification step. R is often referred to as the weight percent gain (WPG) in literature. The correction $(1 + R)$ is needed to compare variously modified specimens (Thybring 2013). The uncertainty in R yields an uncertainty in c_{acc} of the modified specimens of less than 2%.

Determination of hydroxyl accessibility by spectroscopy was done using a Bruker Tensor 27 ATR-FTIR spectrometer (Bruker Optik GmbH, Fällanden, Switzerland) at ETH Zürich. Vacuum-dried (65 °C, 0 mbar, 24 h) specimens were put in reaction flasks in batches of 7 specimens and vacuum applied for 30 min. Hereafter, 40 mL liquid D_2O (99.9%-atom purity, Sigma Aldrich Chemie GmbH Buchs, Switzerland) were injected with a syringe and vacuum pumping continued for 60 min before pressure equilibration with dry nitrogen gas. After 120 min at atmospheric pressure, the D_2O was exchanged for a fresh batch of 40 mL for overnight soaking followed by vacuum-drying (65 °C, 0 mbar, 24 h). After pressure equilibration with dry nitrogen gas, specimens were transported in glass containers with desiccant (molecular sieves 3 Å, Sigma Aldrich Chemie GmbH, Buchs, Switzerland) to the ATR-FTIR. Here, specimens were split in the middle with a razor blade and swiftly transferred to the ATR crystal for data acquisition (64 scans, range 400–4000 cm^{-1}, 60 s duration). Although the handling of specimens after cutting was swift some of the deuterium exchanged hydroxyls may be re-protonated by contact with air humidity. Tarmian et al. (2017) examined this re-protonation and their results show that the relative hydroxyl accessibility initially decreases in laboratory climate by about 1% per minute after cutting. All acquired IR spectra were analysed using OPUS Version 7.2 (Bruker Optik GmbH, Fällanden, Switzerland). Spectra were baseline corrected using the concave rubberband method (10 iterations, 64 baseline points) and max–min normalised. Hydroxyl accessibility was determined as peak area ratio of deuterated hydroxyl stretching in modified specimens to that in untreated specimens. This was done in order to compare the various modifications, since the total hydroxyl content was reduced to different degrees.

The peak area was calculated as twice the area between 2700 cm^{-1} and the wavenumber of the maximum peak height (around 2510 cm^{-1}). This was done to avoid contributions from CO_2 vibrations found around 2300–2400 cm^{-1}.

Water within wood cell walls

The uptake of moisture under water vapour conditions was experimentally characterised using the same DVS-ET1 equipment and sample preparation method used for hydroxyl accessibility determination. Initially, each specimen (5–10 mg) of either earlywood or latewood was dried at 60 °C for 6 h followed by a 1 h thermal stabilisation period. Hereafter, the specimen was exposed to increasing levels of H_2O vapour pressure in steps of 10% relative humidity. During each step, the change in mass was recorded until a selected quasi-equilibrium condition of 0.0005% min^{-1} for 10 min. (5 μg g^{-1} min^{-1}) was met. This may produce a deviation from the true equilibrium of about 1% moisture content (Glass et al. 2018), which corresponds with 0.56 mmol g^{-1} water.

Additionally, the cell wall moisture capacity was analysed by differential scanning calorimetry (DSC Q2000, TA instruments, Germany) (Zauer et al. 2014). Specimens were first water-saturated using vacuum impregnation (0–1 mbar for 5 min. followed by injection of water while pumping for 1 min.). Hereafter, specimens were left to soak for 60 min at saturation pressure and overnight soaking at atmospheric pressure. From this saturated material, small specimens (1–7 mg) were cut with a razor blade, put into Tzero aluminium pans (TA Instruments) and hermetically sealed. All pans were weighed to a resolution of 0.01 mg before and after specimens were inserted. The cell wall moisture capacity was determined by equilibrating the sealed specimens at − 20 °C for 5 min. and then increasing the temperature to 20 °C at a rate of 2 °C min^{-1}. This cycle was run two times for each specimen followed by determination of dry masses after drying specimen and pans in vacuum oven (65 °C, 0 mbar) for 24 h. From measured total energy of melting (Q) in a temperature interval visually picked from the heating curves, dry wood mass (m_0) and the total specimen mass (m_{tot}), the cell wall moisture capacity, $u_{cw,max}$ was calculated as:

$$u_{\text{cw,max}} = \frac{m_{\text{tot}} - m_0 - \left(\frac{Q}{H_f}\right)}{m_0} \qquad (3)$$

where H_f is the enthalpy of fusion of water of 333.7 J g^{-1} (Lide 2013). The first two terms in the numerator of Eq. (3) represent the total water mass in the specimen, while the last term in brackets calculates the freezable water which is found outside cell walls (Fredriksson and Thybring 2019). Calibration of the DSC Q2000 for enthalpy of fusion was done with deionised water (melting point 0 °C, enthalpy of fusion 333.7 J g^{-1}).

All moisture contents and cell wall moisture uptake capacities were corrected for mass gain during the modification step by multiplication with $(1 + R)$ (Thybring 2013). The uncertainty in R yields an uncertainty in moisture content and capacity for the modified specimens of less than 2%. From the moisture content and capacity results, the moisture exclusion efficiency was determined as the reduction in moisture content in modified specimens relative to that in unmodified control specimens. For the vapour conditioned wood, the deviation from true equilibrium results in an error in absolute moisture exclusion of less than 5% on average over the hygroscopic range.

Results and discussion

Chemistry in untreated and modified cell walls

While previous studies in literature have applied Raman spectroscopy to investigate various chemical wood modifications, it is only within the last decade that Raman imaging has been used to obtain both spectral and spatial information on modified wood (Cabane et al. 2014, 2016; Ermeydan et al. 2012, 2014a; Frey et al. 2018; Keplinger et al. 2015; Olaniran et al. 2019).

In Fig. 2, the distribution of bond stretching vibrations of C=O and C–H in the untreated and variously modified wood is shown based on identification of these Raman vibrations in literature (Agarwal 1999; Larkin 2011). These two chemical bonds are characteristic for all three modifications. The intensity scale is similar across the different wood specimens for each bond vibration, and it is therefore clear that the modifications increase the vibrational intensity of
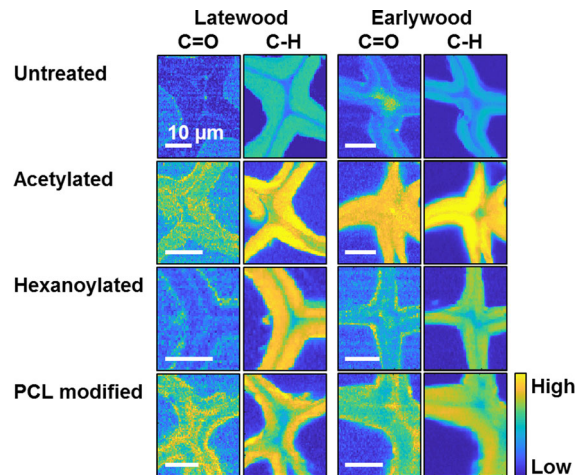

Fig. 2 Distribution of the intensity in the integration bands of C=O stretching vibrations (1720–1740 cm^{-1}) and C-H stretching vibrations (2934–2943 cm^{-1}) in untreated and modified Norway spruce latewood and earlywood. The scale bar is 10 μm

C=O and C–H stretching vibrations throughout the cell wall thickness. In both the untreated and modified wood, the intensity is lower in the lignin-rich cell corners and middle lamellae, but modification is seen to be present also in these regions. At the lumen-cell wall surfaces the vibrational intensity of both C=O and C–H bonds appears slightly increased, indicating a more intense modification of these surfaces than the internal parts of the cell walls. Overall, Fig. 2 shows that the major part of the cell walls has been modified. See more details in the *Supplementary Material*.

Effect of modification on hydroxyl accessibility

Figure 3a shows the gravimetrically determined hydroxyl accessibility in earlywood as function of mass gain of the various modifications. Fewer levels of modification in latewood were examined, however, the results show the same trend although latewood has a higher hydroxyl accessibility in the untreated state (Thybring et al. 2017), see *Supplementary Material*. The trends in the gravimetrically determined data are confirmed by the spectroscopically determined accessibilities in Fig. 3b, although the uncertainty in this method is larger (Tarmian et al. 2017). A large variability between modifications in their effect on the hydroxyl accessibility is seen. By linear regression of the accessibilities for acetylated and hexanoylated specimens in Fig. 3a, crossing the ordinate at the value
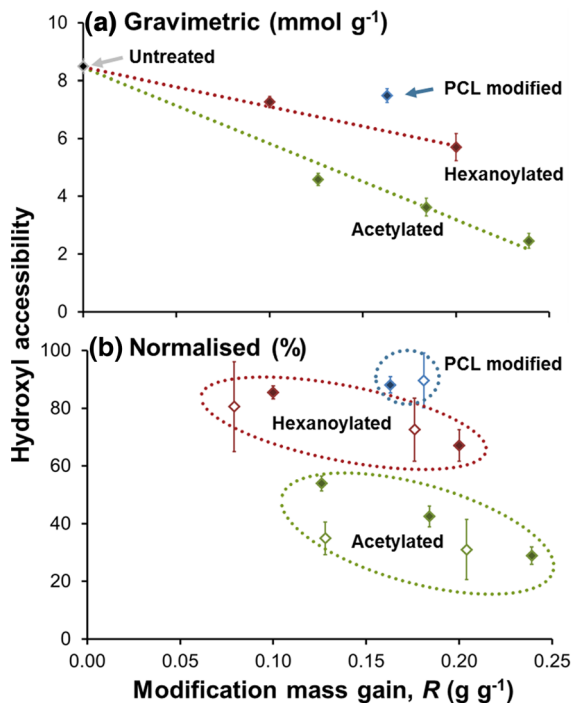
Fig. 3 Hydroxyl accessibility in modified earlywood of Norway spruce as function of mass gain given by **a** gravimetrically determined hydroxyl accessibility (in mmol g^{-1}) and **b** normalised with the accessibility measured for untreated wood where unfilled diamonds mark spectroscopically determined accessibilities and filled diamonds mark gravimetrically determined accessibilities

for untreated wood, the decrease in accessibility per gram added mass is found for the two modifications, see Table 3.

At the same time, PCL modification to $R = 0.163$ decreases the hydroxyl accessibility by 1.0 mmol g^{-1} corresponding to a reduction of 6.2 mmol per gram mass gain. The uncertainty in R causes an uncertainty of 10% on the inclination of the linear regression lines.

This is taken into account in the values reported in Table 3.

Acetylation exhibits the highest reduction in hydroxyl accessibility per mass gain, which is not surprising given that acetylation substitutes the most hydroxyls per mass gain of the three modifications. Thus, hexanoylation reduces the hydroxyl accessibility by about half as much as acetylation for similar mass gain. While PCL modification does not change the amount of hydroxyls due to the carboxyl functionality at the end of each functional group, it nevertheless reduces the accessibility by about half as much as hexanoylation.

All three modifications were found to decrease the accessibility more than theoretically estimated from the substitution of hydroxyls within cell walls, see Table 3. This additional reduction could very well be from shielding of remaining hydroxyls within the cell walls as indicated by the reduction in hydroxyl accessibility from PCL modification even though no hydroxyl functionality is lost from this modification. The difference between theoretically estimated hydroxyl substitution and determined hydroxyl reduction increases in the order: acetylation, hexanoylation, PCL modification, see Table 3. Both hexanoylation and PCL modification add functional groups with a molecular volume, V_{sub} which is more than 2.5 times larger than that added by acetylation, see Table 1. It is therefore tempting to ascribe the larger shielding effect of the previous modifications to molecular size. However, the added volume per mass gain does not correlate with the supposed shielding effect, since PCL modification adds the smallest volume and hexanoylation the largest for similar mass gain of the three modifications as seen in Table 1. The underlying cause for the effect of modification on hydroxyl

Table 3 Theoretically estimated hydroxyl substitution from Table 1 along with measured change in hydroxyl accessibility per gram added mass of the various modifications

Modification	Theoretical Δc_{sub} (mmol g^{-1})	Determined $\Delta c_{sub} + \Delta c_{shield}$ (mmol g^{-1})	Difference Δc_{shield} (mmol g^{-1})	Rel. difference $\Delta c_{shield}/(\Delta c_{sub} + \Delta c_{shield})$ (mmol g^{-1})
Acetylation	23.8	24.1–26.5	0.3–2.7	app. 1–10%
Hexanoylation	10.2	12.4–13.6	2.2–3.4	app. 18–25%
PCL modification	0.0	5.6–6.2	5.6–6.2	100%

For the determined $\Delta c_{sub} + \Delta c_{shield}$ the interval corresponds to an underestimation in of R of 10%

accessibility beyond substitution remains therefore unknown.

Effect of modification on cell wall moisture

Figure 4 shows the cell wall moisture content in the untreated and modified earlywood under both hygroscopic (water vapour) conditions and at water-saturation. The moisture content in the modified wood has been corrected for mass gain due to the modification as described in Materials and Methods. Traditionally, wood moisture content is reported in literature as water mass per dry wood mass, i.e. g g^{-1}. However, in this study the moisture content is given in mmol water molecules per gram dry wood mass to illustrate potential correlations with the hydroxyl accessibility, which has the same unit.

All three modifications are seen in Fig. 4 to reduce the amount of moisture within the cell walls. From these data, the moisture exclusion efficiency of each modification at each mass gain is determined. This efficiency is shown in Fig. 5a as function of the
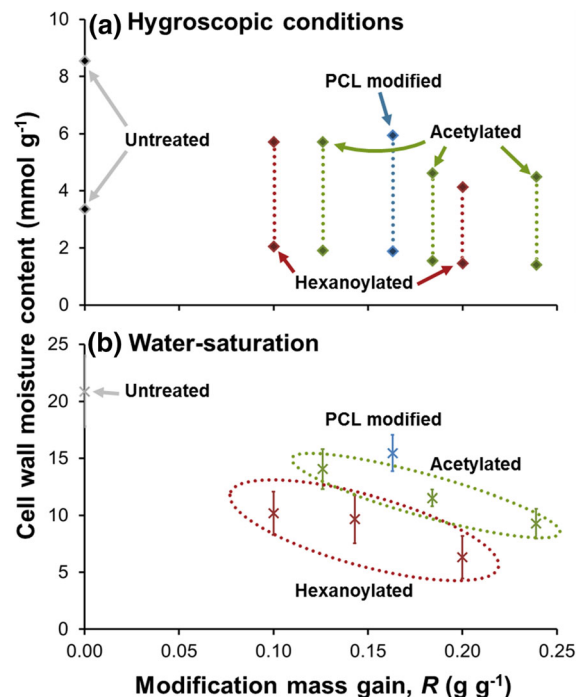

Fig. 5 a Moisture exclusion efficiency of modified earlywood cell walls of Norway spruce, i.e. relative reduction in cell wall moisture content compared with untreated wood, as function of **a** gravimetrically determined hydroxyl accessibility, **b** added molecular volume. Results are shown both for hygroscopic moisture content (filled diamonds) and at water-saturation (open diamonds)

hydroxyl accessibility. From this it is clear that the accessibility of water to hydroxyls confined in solid cell walls do not control the moisture content, since similar moisture exclusion efficiencies can be found in modified materials with a large disparity in hydroxyl accessibility. This contradicts the hypothesis of Papadopoulos and Hill (2003) that reaction with differently sized anhydrides to the same degree results in similar moisture exclusion efficiencies because of equal reductions in hydroxyl accessibility by combined substitution and shielding. Instead, Fig. 5b points to another mechanism behind moisture uptake in solid wood cell walls, which is spatial confinement. It is well-known that dimensional changes of wood as a result of moisture changes involve the built-up or release of internal stresses within the material (Tarkow and Turner 1958). Thus, moisture uptake is accompanied by swelling of the solid cell walls which is restrained by the build-up of mechanical energy

Fig. 4 Moisture content (in mmol g^{-1}) within cell walls of untreated and modified earlywood as function of modification mass gain under **a** hygroscopic conditions (upper data points at 80% RH, lower data points at 30% RH), **b** fully water-saturated conditions
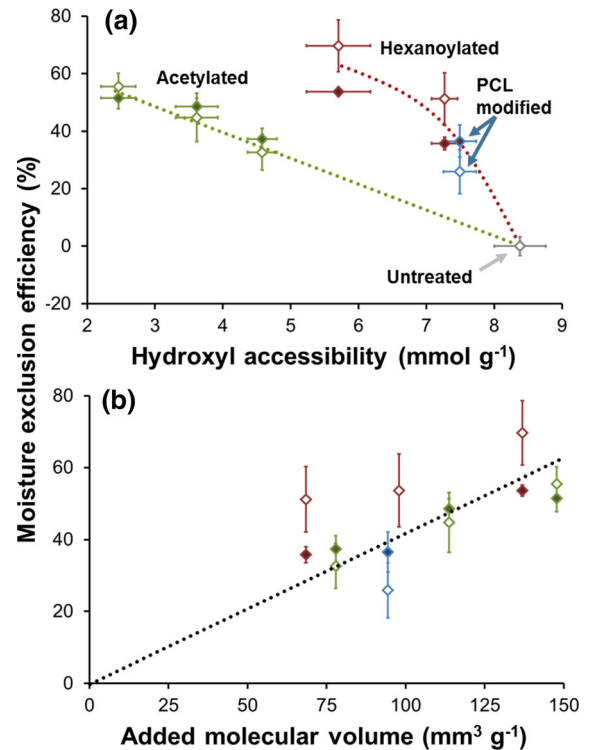
(Bertinetti et al. 2013, 2016). Reacting bulky molecules with the constituent cell wall polymers pre-swells the cell walls and at the same time reduces the available space for water. This leads to a lower moisture content at specific environmental conditions, i.e. moisture exclusion, which is correlated with the total molecular volume of added functional groups within cell walls as seen in Fig. 5b. However, some differences are seen between water-saturated and hygroscopic conditions between acetylated and hexanoylated wood. Acetylation excludes moisture from cell walls relative to untreated wood to a similar degree at saturation and under hygroscopic conditions, while hexanoylation appears to exclude moisture better at water-saturation. This is opposite to the results by Papadopoulos et al. (2004) on Corsican pine which indicate that hexanoylation creates a larger void volume within cell walls than acetylation. The void volume is supposedly mostly available for moisture in the saturated state, which would decrease moisture exclusion compared with hygroscopic conditions. This is, however, not what the results in Fig. 5 show. For Scots pine, however, no significant difference between acetylation and hexanoylation was found (Papadopouls 2001), pointing to differences between wood species in how they react to modification. The correlation between moisture exclusion under hygroscopic conditions and the added molecular volume in Fig. 5b is in line with results for wood reacted with various sizes of carboxylic acid anhydrides (Hill and Jones 1996; Papadopoulos and Hill 2003) as seen in the literature data depicted in the *Supplementary Material*. For the first time, however, this study shows that moisture exclusion cannot predominantly depend on shielding of hydroxyls as large differences in hydroxyl accessibility to water may exist in modified wood cell walls.

Conclusion

Norway spruce wood was treated by three different chemical modifications: acetylation, hexanoylation, and polycaprolactone (PCL) modification. All modifications were found to modify the cell wall chemistry across the cell wall thickness. The modifications reduced the hydroxyl accessibility of the wood for water which could only be partly explained by hydroxyl substitution, and additional contributions

from shielding of hydroxyl were speculated. The moisture content of the wood was reduced by modification. However, the reduction in moisture was clearly shown not to correlate with the hydroxyl accessibility of the material. Instead, the molecular volume of the added functional groups by modification was shown to control the reduction in moisture content, pointing to spatial confinement as the underlying mechanism for moisture uptake in wood.

References

Agarwal UP (1999) An overview of Raman spectroscopy as applied to lignocellulosic materials. In: Argyropoulos DS (ed) Advances in lignocellulosics characterization. Tappi Press, Atlanta, pp 201–225

Altgen M, Willems W, Hosseinpourpia R, Rautkari L (2018) Hydroxyl accessibility and dimensional changes of Scots pine sapwood affected by alterations in the cell wall ultrastructure during heat-treatment. Polym Degrad Stabil 152:244–252. https://doi.org/10.1016/j.polymdegradstab.2018.05.005

Berthold J, Desbrieres J, Rinaudo M, Salmén L (1994) Types of adsorbed water in relation to the ionic groups and their counterions for some cellulose derivatives. Polymer 35:5729–5736. https://doi.org/10.1016/S0032-3861(05)80048-5

Berthold J, Rinaudo M, Salmén L (1996) Association of water to polar groups; estimations by an adsorption model for lignocellulosic materials. Colloid Surface A 112:117–129. https://doi.org/10.1016/0927-7757(95)03419-6

Berthold J, Olsson RJO, Salmén L (1998) Water sorption to hydroxyl and carboxylic acid groups in carboxymethyl-cellulose (CMC) studied with NIR-spectroscopy. Cellulose 5:281–298. https://doi.org/10.1023/A:1009298907734

Bertinetti L, Fischer FD, Fratzl P (2013) Physicochemical basis for water-actuated movement and stress generation in nonliving plant tissues. Phys Rev Lett 111:238001. https://doi.org/10.1103/PhysRevLett.111.238001

Bertinetti L, Fratzl P, Zemb T (2016) Chemical, colloidal and mechanical contributions to the state of water in wood cell walls. New J Phys 18:083048. https://doi.org/10.1088/1367-2630/18/8/083048

Bro R, De Jong S (1997) A fast non-negativity-constrained least squares algorithm. J Chemometr 11:393–401. https://doi.org/10.1002/(sici)1099-128x(199709/10)11:5%3c393:aid-cem483%3e3.0.co;2-l

Cabane E, Keplinger T, Künniger T, Merk V, Burgert I (2016) Functional lignocellulosic materials prepared by ATRP

from a wood scaffold. Sci Rep 6:31287. https://doi.org/10.1038/srep31287

Cabane E, Keplinger T, Merk V, Hass P, Burgert I (2014) Renewable and functional wood materials by grafting polymerization within cell walls. Chemsuschem 7:1020–1025. https://doi.org/10.1002/cssc.201301107

Eilers PHC (2004) Parametric time warping. Anal Chem 76:404–411. https://doi.org/10.1021/ac034800e

Ermeydan MA, Cabane E, Gierlinger N, Koetz J, Burgert I (2014a) Improvement of wood material properties via in situ polymerization of styrene into tosylated cell walls. RSC Adv 4:12981–12988. https://doi.org/10.1039/C4RA00741G

Ermeydan MA, Cabane E, Hass P, Koetz J, Burgert I (2014b) Fully biodegradable modification of wood for improvement of dimensional stability and water absorption properties by poly([varepsilon]-caprolactone) grafting into the cell walls. Green Chem 16:3313–3321. https://doi.org/10.1039/C4GC00194J

Ermeydan MA, Cabane E, Masic A, Koetz J, Burgert I (2012) Flavonoid insertion into cell walls improves wood properties. ACS Appl Mater Inter 4:5782–5789. https://doi.org/10.1021/am301266k

Fredriksson M, Thybring EE (2019) On sorption hysteresis in wood: separating hysteresis in cell wall water and capillary water in the full moisture range. PLoS ONE 14:e0225111. https://doi.org/10.1371/journal.pone.0225111

Frey M, Widner D, Segmehl JS, Casdorff K, Keplinger T, Burgert I (2018) Delignified and densified cellulose bulk materials with excellent tensile properties for sustainable engineering. ACS Appl Mater Inter 10:5030–5037. https://doi.org/10.1021/acsami.7b18646

Gibbons GC (1953) The moisture regain of methylcellulose and cellulose acetate. J Text I T 44:T201–T208. https://doi.org/10.1080/19447025308659739

Gierlinger N, Keplinger T, Harrington M (2012) Imaging of plant cell walls by confocal Raman microscopy. Nat protoc 7:1694–1708. https://doi.org/10.1038/nprot.2012.092

Glass SV, Boardman CR, Thybring EE, Zelinka SL (2018) Quantifying and reducing errors in equilibrium moisture content measurements with dynamic vapor sorption (DVS) experiments. Wood Sci Technol 52:909–927. https://doi.org/10.1007/s00226-018-1007-0

Gold V, Satchell DPN (1955) The principles of hydrogen isotope exchange reactions in solution. Q Rev Chem Soc 9:51–72. https://doi.org/10.1039/qr9550900051

Guthrie JD, Heinzelman DC (1974) Deuterium-hydrogen-exchange accessibility of cellulose by use of D_2O–18 and mass-spectroscopy. Text Res J 44:981–985. https://doi.org/10.1177/004051757404401214

Hill CAS, Jones D (1996) The dimensional stabilisation of Corsican pine sapwood by reaction with carboxylic acid anhydrides: the effect of chain length. Holzforschung 50:457–462. https://doi.org/10.1515/hfsg.1996.50.5.457

Hill CAS, Curling SF, Kwon JH, Marty V (2009) Decay resistance of acetylated and hexanoylated hardwood and softwood species exposed to Coniophora puteana. Holzforschung 63:619–625. https://doi.org/10.1515/HF.2009.124

Hofstetter K, Hinterstoisser B, Salmén L (2006) Moisture uptake in native cellulose—the roles of different hydrogen

bonds: a dynamic FT-IR study using deuterium exchange. Cellulose 13:131–145. https://doi.org/10.1007/s10570-006-9055-2

Howsmon JA (1949) Water sorption and the poly-phase structure of cellulose fibers. Text Res J 19:152–163. https://doi.org/10.1177/004051754901900303

Jaumot J, Gargallo R, de Juan A, Tauler R (2005) A graphical user-friendly interface for MCR-ALS: a new tool for multivariate curve resolution in MATLAB. Chemometr Intell Lab 76:101–110. https://doi.org/10.1016/j.chemolab.2004.12.007

Keplinger T, Cabane E, Chanana M, Hass P, Merk V, Gierlinger N, Burgert I (2015) A versatile strategy for grafting polymers to wood cell walls. Acta Biomater 11:256–263. https://doi.org/10.1016/j.actbio.2014.09.016

Larkin P (2011) Illustrated IR and Raman spectra demonstrating important functional groups. In: Larkin P (ed) Infrared and Raman spectroscopy. Elsevier, Oxford, pp 135–176. https://doi.org/10.1016/B978-0-12-386984-5.10008-4

Lide DR (2013) Enthalpy of fusion. In: Haynes WM (ed) CRC handbook of chemistry and physics, 94th edition (internet version) edn. CRC Press/Taylor and Francis, Boca Raton, pp 146–155

Lindh EL, Bergenstråhle-Wohlert M, Terenzi C, Salmén L, Furó I (2016) Non-exchanging hydroxyl groups on the surface of cellulose fibrils: the role of interaction with water. Carbohydr Res 434:136–142. https://doi.org/10.1016/j.carres.2016.09.006

Mann J, Marrinan HJ (1956) The reaction between cellulose and heavy water 1. A qualitative study by infra-red spectroscopy. Trans Faraday Soc 52:481–487. https://doi.org/10.1039/TF9565200481

Olaniran SO, Etienne C, Keplinger T, Olufemi B, Rüggeberg M (2019) Mechanical behaviour of acetylated rubber wood subjected to artificial weathering. Holzforschung 73:1005. https://doi.org/10.1515/hf-2018-0274

Papadopouls AN (2001) Swelling, cell wall porosity and chemical modification of wood. Ph.D. Thesis, University of Wales Bangor, pp 285

Papadopoulos AN, Hill CAS (2003) The sorption of water vapour by anhydride modified softwood. Wood Sci Technol 37:221–231. https://doi.org/10.1007/s00226-003-0192-6

Papadopoulos AN, Hill CAS, Gkaraveli A (2004) Analysis of the swelling behaviour of chemically modified softwood: a novel approach. Holz Roh Werkst 62:107–112. https://doi.org/10.1007/s00107-003-0448-8

Piqueras S, Duponchel L, Tauler R, de Juan A (2011) Resolution and segmentation of hyperspectral biomedical images by Multivariate Curve Resolution-Alternating Least Squares. Anal Chim Acta 705:182–192. https://doi.org/10.1016/j.aca.2011.05.020

Popescu CM, Hill CAS, Curling S, Ormondroyd GA, Xie Y (2014) The water vapour sorption behaviour of acetylated birch wood: how acetylation affects the sorption isotherm and accessible hydroxyl content. J Mater Sci 49:2362–2371. https://doi.org/10.1007/s10853-013-7937-x

Rautkari L, Hill CAS, Curling S, Jalaludin Z, Ormondroyd GA (2013) What is the role of the accessibility of wood hydroxyl groups in controlling moisture content? J Mater

Sci 48:6352–6356. https://doi.org/10.1007/s10853-013-7434-2

Rousselle MA, Nelson ML (1971) Accessibility of cotton cellulose by deuterium exchange. Text Res J 41:599–604. https://doi.org/10.1177/004051757104100708

Schmidt M, Gierlinger N, Schade U, Rogge T, Grunze M (2006) Polarized infrared microspectroscopy of single spruce fibers: hydrogen bonding in wood polymers. Biopolymers 83:546–555. https://doi.org/10.1002/bip.20585

Sepall O, Mason SG (1961) Hydrogen exchange between cellulose and water 1. Measurement of accessibility. Can J Chem 39:1934–1943. https://doi.org/10.1139/v61-260

Slonimskii GL, Askadskii AA, Kitaigorodskii AI (1970) The packing of polymer molecules. Polym Sci USSR 12:556–577. https://doi.org/10.1016/0032-3950(70)90345-X

Stevens CV, Smith BF (1970) Crosslinking cotton cellulose with ethyleneurea derivatives having varying hydrogen-bonding capabilities. II Accessibility determinations. J Appl Polym Sci 14:1691–1700. https://doi.org/10.1002/app.1970.070140704

Taniguchi T, Harada H, Nakato K (1966) Accessibility of hydroxyl groups in wood. Mokuzai Gakkaishi 10:215–220

Tarkow H, Turner HD (1958) The swelling pressure of wood. Forest Prod J 8:193–197

Tarmian A, Burgert I, Thybring EE (2017) Hydroxyl accessibility in wood by deuterium exchange and ATR-FTIR spectroscopy: methodological uncertainties. Wood Sci Technol 51:845–853. https://doi.org/10.1007/s00226-017-0922-9

Thybring EE (2013) The decay resistance of modified wood influenced by moisture exclusion and swelling reduction. Int Biodeter Biodegr 82:87–95. https://doi.org/10.1016/j.ibiod.2013.02.004

Thybring EE, Thygesen LG, Burgert I (2017) Hydroxyl accessibility in wood cell walls as affected by drying and re-wetting procedures. Cellulose 24:2375–2384. https://doi.org/10.1007/s10570-017-1278-x

Tjeerdsma BF, Boonstra M, Pizzi A, Tekely P, Militz H (1998) Characterisation of thermally modified wood: molecular reasons for wood performance improvement. Holz Roh Werkst 56:149–153. https://doi.org/10.1007/s001070050287

Wadehra IL, Manley RS (1966) Accessibility of hydrocelluloses and oligosaccharides by hydrogen exchange. Makromolekul Chem 94:42–51. https://doi.org/10.1002/macp.1966.020940105

Watanabe A, Morita S, Kokot S, Matsubara M, Fukai K, Ozaki Y (2006) Drying process of microcrystalline cellulose studied by attenuated total reflection IR spectroscopy with two-dimensional correlation spectroscopy and principal component analysis. J Mol Struct 799:102–110. https://doi.org/10.1016/j.molstruc.2006.03.018

Zauer M, Kretzschmar J, Großmann L, Pfriem A, Wagenführ A (2014) Analysis of the pore-size distribution and fiber saturation point of native and thermally modified wood using differential scanning calorimetry. Wood Sci Technol 48:177–193. https://doi.org/10.1007/s00226-013-0597-9